



Mono- and dinuclear luminescent 1,1'-biisoquinoline gold(I) complexes

Manuel Bardají*, Ana B. Miguel-Coello, Pablo Espinet*

IU CINQUIMA/Química Inorgánica, Facultad de Ciencias, Universidad de Valladolid, E-47071 Valladolid, Spain

ARTICLE INFO

Article history:

Received 29 March 2012

Accepted 13 June 2012

Available online 23 June 2012

Keywords:

Biisoquinoline

Gold

Gold–gold contact

Luminescence

Monodentate ligand

Bridging ligand

ABSTRACT

Mono- and dinuclear, cationic or neutral gold(I) derivatives $[(\text{biisoq})(\text{AuL})]^{n+}$ ($\text{L} = \text{PPh}_3$, $n = 1$; $\text{L} = \text{C}_6\text{F}_5$, $n = 0$), and $[(\mu\text{-biisoq})(\text{AuL})_2]^{n+}$ ($\text{biisoq} = 1,1'\text{-biisoquinoline}$; $\text{L} = \text{PMe}_3$, PPh_3 , PMePh_2 , $n = 2$; $\text{L} = \text{C}_6\text{F}_5$, $n = 0$) have been prepared. Auophilic interactions and steric requirements of the co-ligand L impose the torsion angle between the two isoquinoline units of the flexible, non-planar 1,1'-biisoquinoline ligand, affording different structures. The X-ray molecular structure of the mononuclear complex with PPh_3 confirmed the monodentate mode for the biisoquinoline ligand. In the three X-ray structures solved for dinuclear compounds with bridging biisoquinoline, the torsion angles and the intramolecular gold–gold distances found are, respectively: 65.2° and $3.0739(7) \text{ \AA}$ for $\text{L} = \text{PMe}_3$; 80.10° and 3.785 \AA for $\text{L} = \text{C}_6\text{F}_5$; 95.6° and 4.505 \AA for $\text{L} = \text{PMePh}_2$. All the phosphine derivatives are luminescent at room temperature in the solid state, with emission maxima in the range 390–422 nm, and emit from 370 to 438 nm at 77 K. They are also emissive in CH_2Cl_2 at 298 K in the range 381–458 nm, whilst they are luminescent at 77 K in the range 382–550 nm. The fluoroaryl derivatives are not emissive.

© 2012 Elsevier B.V. All rights reserved.

1. Introduction

The study of closed shell gold(I) derivatives has revealed the frequent presence of short gold–gold distances, which have been attributed to correlation effects reinforced by relativistic effects and electrostatic contributions. The so-called auophilic interaction leads to gold–gold distances in the range 2.8–3.6 Å, with strength similar to some hydrogen bonds, in the order 20–50 kJ/mol [1]. Gold(I) usually forms two-coordinated complexes displaying linear geometry, which facilitates the formation of these gold–gold contacts, provided the steric requirements of the ligands do not hinder the interaction. Many gold(I) compounds, with or without gold–gold contacts, are luminescent in the visible region [2], and some of them have been proposed for applications as chemosensors for cations or anions, or as light-emitting diodes [3].

Ligands incorporating a 1,1'-binaphthyl unit, for instance chiral N-heterocyclic carbenes, have been receiving attention recently because of their application in catalytic asymmetric reactions [4]. These ligands can show optical activity based on the high barrier to rotation about the C–C σ -bond, which gives rise to atropisomers [5]. In particular, 1,1'-biisoquinoline is a diamine with a more extended π -acceptor system than 2,2'-bipyridine, while it has a comparable N σ -donor ability. 1,1'-Biisoquinoline is non-planar, as result of trans-annular steric hindrance between the hydrogen atoms in positions 8 and 8', one on each isoquinoline subunit (see labels in Scheme 1 below). Its lack of planarity might be

thought to disfavor its chelating coordination, but in fact this flexible ligand usually acts as chelate in metal complexes, as reported for square planar Rh(I) [6] and Pt(II) [7], or octahedral Os(II) [8], Ru(II) [8,9], and Ir(III) complexes [10]. Potentially 1,1'-biisoquinoline can also act as bridging bidentate and as monodentate ligand, although, among the many reported complexes, only two reports of 1,1'-biisoquinoline acting as a bridging ligand (a dinuclear palladium complex [11] and a series of silver(I) compounds recently described by us [12]), and only one complex where it is acting as monodentate ligand (the X-ray crystal structure of a platinum complex), are found [7a].

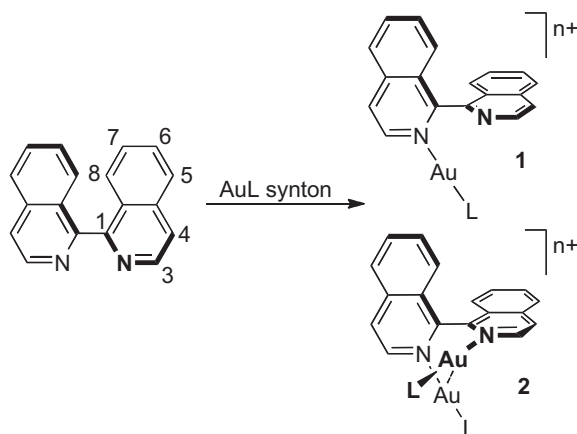
The predominant tendency of 1,1'-biisoquinoline to behave as a chelate ligand should be frustrated on metal centers with linear coordination, thus favoring the occurrence of the other bonding modes. In effect, in this paper we report mono- and dinuclear gold(I) compounds with the 1,1'-biisoquinoline ligand acting as monodentate or bridging bidentate, respectively. Most of the complexes are luminescent, both in solution and in the solid state.

2. Experimental

IR spectra were recorded on a FT 1720X Perkin-Elmer spectrophotometer ($4000\text{--}400 \text{ cm}^{-1}$) using KBr pellets. ^1H , ^{19}F and $^{31}\text{P}\{^1\text{H}\}$ NMR spectra were recorded on Bruker AC-300, ARX-300 or AV-400 instruments in CDCl_3 solutions (if no other solvent is stated); chemical shifts are quoted relative to SiMe_4 (external, ^1H), CFCl_3 (external, ^{19}F) and 85% H_3PO_4 (external, ^{31}P). ^1H NMR labels are in Scheme 1. Elemental analyses were performed with a Perkin-Elmer 2400 microanalyzer. Emission and excitation spectra

* Corresponding authors. Tel.: +34 983184624; fax: +34 983423013.

E-mail addresses: bardaji@qi.uva.es (M. Bardají), espinet@qi.uva.es (P. Espinet).



Scheme 1.

at 298 and 77 K were measured in the solid state as finely pulverized KBr mixtures, and in deoxygenated CH_2Cl_2 solutions in quartz tubes with a Perkin-Elmer LS-55 spectrofluorimeter. UV-Vis absorption spectra were recorded at 297 K on a Shimadzu UV-2550. Literature methods were used to prepare 1,1'-biisoquinoline [9f], $[\text{AuCl}(\text{PRR}'_2)]$ [13], and $[\text{Au}(\text{C}_6\text{F}_5)(\text{tht})]$ [14].

2.1. Synthesis of $[(\mu\text{-biisoq})\{\text{Au}(\text{PRR}'_2)\}_2](\text{CF}_3\text{SO}_3)_2$; $R = R' = \text{Me}$ **2a**, Ph **2b**; $R = \text{Me}$, $R' = \text{Ph}$ **2c**

To an acetone solution (20 mL) of $[\text{AuCl}(\text{PRR}'_2)]$ (0.17 mmol; $R = R' = \text{Me}$ 52 mg, Ph 84 mg; $R = \text{Me}$, $R' = \text{Ph}$ 74 mg) was added $\text{Ag}(\text{CF}_3\text{SO}_3)$ (44 mg, 0.17 mmol), and the reaction stirred for 60 min protected from the light. AgCl was filtered off, and the corresponding biisoquinoline (22 mg, 0.085 mmol) was added to the solution. After stirring for 1 h, the suspension was concentrated to ca. 5 mL. Addition of diethyl ether afforded compounds **2a–2c** as white solids. Yield of **2a**: 61 mg, 65%. *Anal. Calc.* for C, 28.38; H, 2.75; N, 2.55. Found: C, 28.65; H, 2.67; N, 2.83%. $^1\text{H NMR}$: δ 1.45 (d, $J_{\text{HP}} = 10.5$ Hz, 18H, Me), 7.48 (d, $J_{\text{HH}} = 8.6$ Hz, 2H, H^8), 7.65 (t, $J_{\text{HH}} = 7.8$ Hz, 2H, H^7), 8.11 (t, $J_{\text{HH}} = 7.5$ Hz, 2H, H^6), 8.13 (d, $J_{\text{HH}} = 8.3$ Hz, 2H, H^5), 8.20 (d, $J_{\text{HH}} = 5.7$ Hz, 2H, H^4), 8.95 (d, $J_{\text{HH}} = 5.7$ Hz, 2H, H^3). $^{19}\text{F NMR}$: δ -78.3 (s). $^{31}\text{P}\{^1\text{H}\}$ NMR: δ -11.2 (s). IR (KBr): 1274, 638 (CF_3SO_3) cm^{-1} . Yield of **2b**: 81 mg, 65%. *Anal. Calc.* for C, 45.66; H, 2.87; N, 1.90. Found: C, 45.32; H, 2.77; N, 1.80%. $^1\text{H NMR}$: δ 7.0–7.5 (m, 32H, $\text{Ph} + \text{H}^8$), 7.75 (t, $J_{\text{HH}} = 7.9$ Hz, 2H, H^7), 8.11 (t, $J_{\text{HH}} = 7.6$ Hz, 2H, H^6), 8.08 (d, $J_{\text{HH}} = 8.0$ Hz, 2H, H^5), 8.27 (d, $J_{\text{HH}} = 6.1$ Hz, 2H, H^4), 9.15 (d, $J_{\text{HH}} = 6.1$ Hz, 2H, H^3). $^{19}\text{F NMR}$: δ -78.3 (s). $^{31}\text{P}\{^1\text{H}\}$ NMR: δ 28.5 (s). IR (KBr): 1260, 640 (CF_3SO_3) cm^{-1} . Yield of **2c**: 79 mg, 69%. *Anal. Calc.* for C, 40.96; H, 2.84; N, 2.08. Found: C, 40.61; H, 2.89; N, 2.0%. $^1\text{H RMN}$: δ 2.04 (d, $J_{\text{HP}} = 11.3$ Hz, 6H, Me), 7.1–7.5 (m, 22H, $\text{Ph} + \text{H}^8$), 7.70 (t, $J_{\text{HH}} = 7.6$ Hz, 2H, H^7), 7.95 (t, $J_{\text{HH}} = 7.8$ Hz, 2H, H^6), 8.08 (d, $J_{\text{HH}} = 8.4$ Hz, 2H, H^5), 8.26 (d, $J_{\text{HH}} = 6.2$ Hz, 2H, H^4), 9.2 (d, $J_{\text{HH}} = 6.2$ Hz, 2H, H^3). $^{19}\text{F NMR}$: δ -78.3 (s). $^{31}\text{P}\{^1\text{H}\}$ NMR: δ 13.9 (s). IR (KBr): 1260, 637 (CF_3SO_3) cm^{-1} .

2.2. Synthesis of $[(\text{biisoq})\{\text{Au}(\text{PPh}_3)\}](\text{CF}_3\text{SO}_3)$ **1b**

To an acetone solution (20 mL) of $[\text{AuCl}(\text{PR}_3)]$ (84 mg, 0.17 mmol) was added $\text{Ag}(\text{CF}_3\text{SO}_3)$ (44 mg, 0.17 mmol), and the reaction stirred for 90 min protected from the light. AgCl was filtered off, and the corresponding biisoquinoline (44 mg, 0.17 mmol) was added to the solution. After stirring for 1 h, the suspension was concentrated to ca. 5 mL. Addition of hexane afforded compounds **1b** as a white solid. Yield of **1b**: 118 mg, 80%. *Anal. Calc.* for C,

51.40; H, 3.15; N, 3.24. Found: C, 51.08; H, 3.27; N, 2.92%. $^1\text{H NMR}$: δ 6.9–7.6 (m, 17H, $\text{Ph} + \text{H}^8$), 7.63 (t, $J_{\text{HH}} = 7.9$ Hz, 2H, H^7), 7.87 (t, $J_{\text{HH}} = 7.6$ Hz, 2H, H^6), 8.05 (d, $J_{\text{HH}} = 8.0$ Hz, 2H, H^5), 8.10 (d, $J_{\text{HH}} = 6.2$ Hz, 2H, H^4), 8.75 (d, $J_{\text{HH}} = 6.2$ Hz, 2H, H^3). $^{19}\text{F NMR}$: δ -78.3 (s). $^{31}\text{P}\{^1\text{H}\}$ NMR: δ 29.7 (s). IR (KBr): 1266, 639 (CF_3SO_3) cm^{-1} .

2.3. Synthesis of $[(\mu\text{-biisoq})\{\text{Au}(\text{C}_6\text{F}_5)_2\}]$ **2d** and $[(\text{biisoq})\{\text{Au}(\text{C}_6\text{F}_5)\}]$ **1d**

To a dichloromethane solution (20 mL) of $[\text{Au}(\text{C}_6\text{F}_5)(\text{tht})]$ (81 mg, 0.18 mmol) was added the stoichiometric amount of the biisoquinoline (23 mg, 0.09 mmol). The resulting solution was stirred for 1 h and concentrated to ca. 5 mL. Addition of hexane afforded the mixture of compounds **2d–1d** as a light yellow solid in 1:2 M ratio. $^1\text{H NMR}$ of **2d**: δ 7.41 (d, $J_{\text{HH}} = 8.6$ Hz, 2H, H^8), 7.69 (t, $J_{\text{HH}} = 7.8$ Hz, 2H, H^7), 8.00 (t, $J_{\text{HH}} = 7.5$ Hz, 2H, H^6), 8.18 (d, $J_{\text{HH}} = 8.3$ Hz, 2H, H^5), 8.29 (d, $J_{\text{HH}} = 5.7$ Hz, 2H, H^4), 8.82 (d, $J_{\text{HH}} = 5.7$ Hz, 2H, H^3). $^{19}\text{F NMR}$ of **2d**: δ -116.59 (m, 4F, $\text{F}_o\text{-Au}$), -159.87 (t, $N = 18.1$ Hz, 2F, $\text{F}_p\text{-Au}$), -163.53 (m, 4F, $\text{F}_m\text{-Au}$). $^1\text{H NMR}$ of **1d**: δ 7.48 (d, $J_{\text{HH}} = 8.6$ Hz, 2H, H^8), 7.56 (t, $J_{\text{HH}} = 7.8$ Hz, 2H, H^7), 7.85 (t, $J_{\text{HH}} = 7.5$ Hz, 2H, H^6), 8.04 (d, $J_{\text{HH}} = 5.7$ Hz, 2H, H^4), 8.06 (d, $J_{\text{HH}} = 8.3$ Hz, 2H, H^5), 8.74 (d, $J_{\text{HH}} = 5.7$ Hz, 2H, H^3). $^{19}\text{F NMR}$ of **1d**: δ -116.59 (m, 4F, $\text{F}_o\text{-Au}$), -160.50 (t, $N = 18.1$ Hz, 2F, $\text{F}_p\text{-Au}$), -163.86 (m, 4F, $\text{F}_m\text{-Au}$).

2.4. Crystal structure determination of compounds **1b**, **2a**, **2c** and **2d**

Crystals of **1b**, **2c** and **2d** were obtained by slow diffusion of hexane into a dichloromethane solution, whilst crystals of **2a** were obtained by slow diffusion of diethyl ether/ethanol into a chloroform solution, always at -18 °C. The crystal was mounted on a glass fiber and transferred to a Bruker SMART CCD diffractometer. Crystal data and details of data collection and structure refinement are given in Table 1. Cell parameters were retrieved using SMART [15] software and refined with SAINT [16] on all observed reflections. Data reduction was performed with the SAINT software and corrected for Lorentz and polarization effects. Absorption corrections were based on multiple scans (program SADABS) [17]. The structure was refined anisotropically on F^2 [18]. All non-hydrogen atomic positions were located in difference Fourier maps and refined anisotropically. The hydrogen atoms were placed in their geometrically generated positions. In the structure of **2c** a water molecule between two positions was included (their H were not added); the CF_3 of one anion is incipiently disordered. The structure of **2d** contains some disordered solvent in the channels, and we were unable to properly model it.

3. Results and discussion

3.1. Synthesis and characterization

The reaction of the 1,1'-biisoquinoline with appropriate gold(I) precursors, prepared in situ, yielded compounds of the types **1** or **2**, according to Scheme 1.

Thus, using $[\text{Au}(\text{CF}_3\text{SO}_3)(\text{PR}_2\text{R}')]_2$, prepared in situ from $[\text{AuCl}(\text{PR}_2\text{R}')]_2$ and $\text{Ag}(\text{CF}_3\text{SO}_3)$, and an Au:1,1'-biisoquinoline 2:1 ratio, the dicationic complexes **2a–c**, with CF_3SO_3 as counter-anion (**2a**: $R = R' = \text{Me}$; **2b**: $R = R' = \text{Ph}$; **2c**: $R = \text{Ph}$, $R' = \text{Me}$), were obtained. Using an Au:1,1'-biisoquinoline 1:1 ratio, the monocationic complex **1b** was obtained. Compounds **1b** and **2a–c** are air-stable white solids at room temperature and were characterized by elemental analysis, and by IR and NMR spectroscopy.

The dicationic complexes **2a–c** show in their $^1\text{H NMR}$ spectra a phosphine:biisoquinoline 2:1 ratio, and only six chemically non-equivalent biisoquinoline protons, as expected for two equivalent

Table 1
Details of crystal data and structure refinement for complexes **1b**, **2a**, **2c** and **2d**.

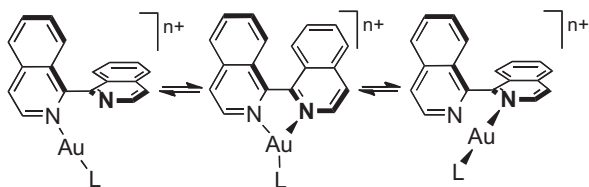
Compound	1b	2a	2c	2d
Empirical formula	C ₃₇ H ₂₇ AuF ₃ N ₂ O ₃ PS	C ₂₆ H ₃₀ Au ₂ F ₆ N ₂ O ₆ P ₂ S ₂	C ₄₆ H ₃₈ Au ₂ F ₆ N ₂ O ₆ P ₂ S ₂ ·H ₂ O	C ₃₀ H ₁₂ Au ₂ F ₁₀ N ₂
FW	864.60	1100.51	1364.78	984.35
T (K)	298(2)	298(2)	298(2)	298(2)
λ (Å)	0.71073	0.71073	0.71073	0.71073
Crystal system	triclinic	orthorhombic	triclinic	monoclinic
Space group	P $\bar{1}$	Pca2(1)	P $\bar{1}$	C2/c
<i>Unit cell dimensions</i>				
a (Å)	12.002(4)	12.948(3)	11.769(8)	16.478(5)
b (Å)	12.384(4)	16.785(4)	13.871(10)	16.319(5)
c (Å)	13.753(5)	16.495(4)	16.878(12)	12.870(4)
α (°)	89.310(7)	90	80.849(12)	90
β (°)	68.336(6)	90	74.947(11)	115.459(5)
γ (°)	63.986(6)	90	67.006(11)	90
V (Å ³)	1679.7(10)	3584.7(14)	2444(3)	3124.9(16)
Z	2	4	2	4
D _{calc} (Mg/m ³)	1.710	2.039	1.854	2.092
Absorption coefficient (mm ⁻¹)	4.546	8.452	6.220	9.460
F(000)	848	2088	1316	1816
Crystal habit	Plate	Needle	Prism	Plate
Crystal size (mm)	0.35 × 0.14 × 0.05	0.38 × 0.09 × 0.07	0.38 × 0.23 × 0.19	0.27 × 0.19 × 0.1
Θ range for data colln	1.62 to 28.33	1.21 to 28.30	1.25 to 28.46	1.85 to 28.32
Index ranges	-16 ≤ h ≤ 15, -16 ≤ k ≤ 16, -17 ≤ l ≤ 18	-17 ≤ h ≤ 17, -22 ≤ k ≤ 22, -22 ≤ l ≤ 21	-15 ≤ h ≤ 15, -18 ≤ k ≤ 18, -22 ≤ l ≤ 22	-21 ≤ h ≤ 21, -21 ≤ k ≤ 21, -17 ≤ l ≤ 17
Reflections collected	16942	34491	24663	15212
Independent reflections	8253 [R _{int} = 0.0440]	8728 [R _{int} = 0.0606]	12068 [R _{int} = 0.0320]	3889 [R _{int} = 0.0641]
Maximum and minimum transmissions	1 and 0.608606	1 and 0.237895	1 and 0.500817	1 and 0.22177
Data/restraints/parameters	8253/0/433	8728/1/421	12068/0/615	3889/0/199
Goodness-of-fit (GOF) on F ²	0.981	1.020	1.015	1.093
Final R indices [I > 2σ(I)]	R ₁ = 0.0410, wR ₂ = 0.0761	R ₁ = 0.0400, wR ₂ = 0.0867	R ₁ = 0.0395, wR ₂ = 0.1004	R ₁ = 0.0408, wR ₂ = 0.1035
R indices (all data)	R ₁ = 0.0739, wR ₂ = 0.0862	R ₁ = 0.0672, wR ₂ = 0.0982	R ₁ = 0.0660, wR ₂ = 0.1135	R ₁ = 0.0747, wR ₂ = 0.1164
Largest difference in peak and hole (e Å ⁻³)	1.303 and -0.509	1.392 and -0.696	1.625 and -1.238	1.826 and -1.129

Table 2
Summary of ¹H NMR resonances of biisoquinoline ligand, either free or coordinated.

Deriv.	H ³	H ⁴	H ⁵	H ⁶	H ⁷	H ⁸
biisoq	8.72	7.82	7.95	7.75	7.50	7.70
2a	8.95	8.20	8.13	8.11	7.65	7.48
2b	9.15	8.27	8.08	8.11	7.75	7.50
2c	9.20	8.26	8.08	7.95	7.70	7.42
1b	8.75	8.10	8.05	7.87	7.63	7.50
2d	8.82	8.29	8.18	8.00	7.69	7.41
1d	8.74	8.04	8.06	7.85	7.56	7.48

halves of the biisoquinoline. These aromatic protons (assigned from COSY experiments) appear low-field shifted by comparison with the free ligand except H⁸, which is high-field shifted (see Table 2). The biggest shifts are found for H⁴ and H³, while the smallest ones are found for H⁵. The ¹⁹F NMR spectra show a singlet at -78.3 ppm, due to the triflate anion. A singlet is observed for **2a-c** in the ³¹P{¹H} NMR spectra, at -11.2 (PMe₃), 28.5 (PPh₃), or 13.9 (PPh₂Me) ppm, respectively.

Compound **1b** shows a phosphine:biisoquinoline 1:1 ratio but the two isoquinoline halves are equivalent in the NMR timescale even at -55 °C, revealing that a very fast fluxional process is

**Scheme 2.**

operating. In addition, a singlet in the ³¹P{¹H} NMR spectra at 29.6 ppm, shifted only by +1.1 ppm compared to derivative **2b**, and a singlet at -78.3 ppm in the ¹⁹F spectra due to the triflate anion, are observed. As for derivatives **2**, the H³-H⁷ resonances are low-field shifted (the biggest shifts are for H⁴, and the smallest one, for H³ is insignificant), whilst H⁸ is high-field shifted, always compared to the free ligand. The actual chemical shift values of **1b** are midway between those for the related complex **2b** and for the free ligand. These NMR features suggest that the fragment Au(PPh₃) is swinging very fast between N and N' (Scheme 2).

The reaction of 1,1'-biisoquinoline with [Au(C₆F₅)(tht)] (tht = tetrahydrothiophene) in Au:biisoquinoline 2:1 ratio yielded an air-stable light yellow solid which proved to be a mixture of the neutral fluoroaryl dinuclear compound **2d** with a bridging biisoquinoline, and the mononuclear compound **1d**. The ¹⁹F NMR spectrum displays two sets of three resonances of close intensity due to the Au-C₆F₅ moiety, in approximately 1:2 ratio, at -116.6, -159.9, and -163.5 ppm for derivative **2d** and at -116.6, -160.5, -163.9 for derivative **1d**, which confirm a mixture of the two compounds. The ¹H NMR spectrum of this mixture displayed only two sets of signals corresponding to the three kinds of isoquinoline moiety in the complexes of Scheme 1, showing that, as observed for **1b**, fast atropisomerization between N and N' is operating in the **1d** component of the mixture. Taking this into account, the mixture **2d:1d** has an approximate 1:2 ratio, and there is no fast biisoquinoline exchange between **2d** and **1d**. This synthesis was monitored in situ, by mixing the starting materials in CDCl₃. At the end of the reaction the ¹⁹F NMR spectrum showed the presence of **1d:2d**:[Au(C₆F₅)(tht)] in 6.7:1:13 ratio. The ¹H NMR spectrum displayed the resonances corresponding to **1d**, **2d** and free biisoquinoline, and also to free and coordinated tht. During the workup, the volatility of tht and the different solubility of the components of the mixture led to the ratio found for the isolated solid,

as discussed above. Different attempts at obtaining pure **1d** or **2d** were frustrating but some microcrystals of **2d**, suitable for X-ray diffraction studies could be picked up from a mixture enriched in **2d**.

3.2. X-ray crystal structure determination of compounds **1b**, **2a**, **2c**, and **2d**

ORTEP representations of the structures of the cations of **1b**, **2a**, and **2c**, and the molecule **2d**, are presented below along with relevant distances and angles. The structures of all the complexes are built around that of the biisoquinoline, which is mostly characterized by the N–C1–C1'–N' torsion angle. This angle sufficiently describes the arrangement of the two halves of the 1,1'-biisoquinoline. On top of this common frame, it is necessary to consider the coordination mode of gold, the possibility of intermolecular Au··Au interactions and, in the dinuclear complexes, the possibility of Au··Au intramolecular interactions.

A theoretical DFT study of free 1,1'-biisoquinoline found that the most stable structure is the *anti* isomer, with a N–C1–C1'–N' torsion angle of 129.9°; its *syn* atropisomer displays a torsion angle of 26.5°, and the calculated atropisomerization barrier is 123.09 kJ/mol [19]. Thus the *anti* atropisomer (dihedral angle > 90°) is preferred for the ligand itself, as found in similar free ligands (101.2° for 8,8'-dimethyl-1,1'-biisoquinoline [20]; 101.6° for 1,1'-biisoquinoline *N,N'*-dioxide [21]). However, the *syn* arrangement (dihedral angle < 90°) is found in metal complexes where the 1,1'-biisoquinoline is acting as a chelate, and the N–C1–C1'–N' torsion angles in those complexes are in the range 20–41° [6–10].

None of the structures studied here show chelating biisoquinoline coordination, nor they show intermolecular Au··Au interactions. Moreover, in all cases the Au coordination is very close to linear, with normal Au–N [22], Au–P, or Au–C₆F₅ [23] distances. Thus the main differential feature of these structures is the N–C1–C1'–N' torsion angle, as the Au–Au distance is a function of this angle, which consequently determines the possibility of Au··Au intradimer auriphilic interactions in the binuclear complexes.

3.2.1. Crystal structure of complex **1b**

Suitable crystals for X-ray studies were obtained by slow diffusion of hexane in a solution of dichloromethane at –18 °C. The corresponding cation is shown in Fig. 1, with selected bond lengths and angles in Table 3. It confirms a mononuclear structure with one monodentate biisoquinoline, for which there is only one precedent

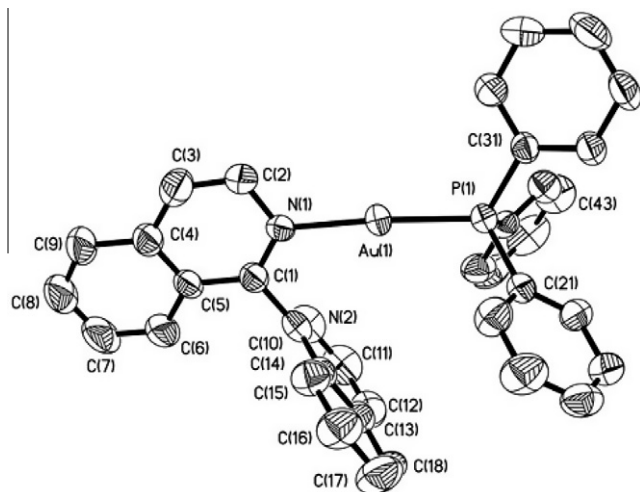


Fig. 1. Structure of the cation of **1b**. Displacement ellipsoids are at 50% probability level (H atoms omitted for clarity).

Table 3
Selected bond lengths (Å) and angles (°) for complex **1b**.

Au(1)–N(1)	2.072(4)	N(1)–Au(1)–P(1)	175.85(11)
Au(1)–P(1)	2.2358(13)	C(31)–P(1)–Au(1)	115.54(16)
N(1)–C(1)	1.320(6)	C(1)–N(1)–C(2)	119.0(4)
P(1)–C(31)	1.805(5)	C(1)–N(1)–C(2)	120.8(3)
N(2)–C(11)	1.358(8)	C(1)–N(1)–Au(1)	120.2(3)

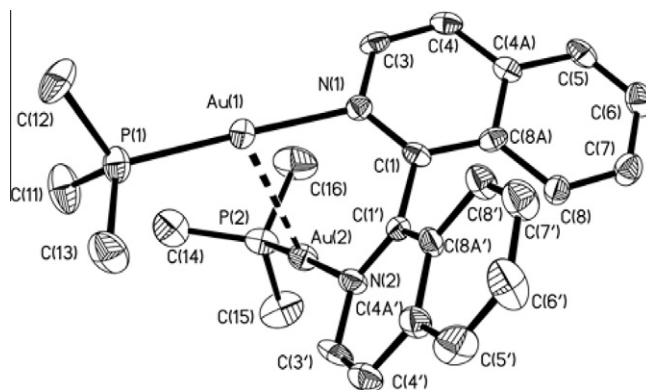


Fig. 2. Structure of the cation of compound **2a**. Displacement ellipsoids are at 25% probability level (H atoms omitted for clarity).

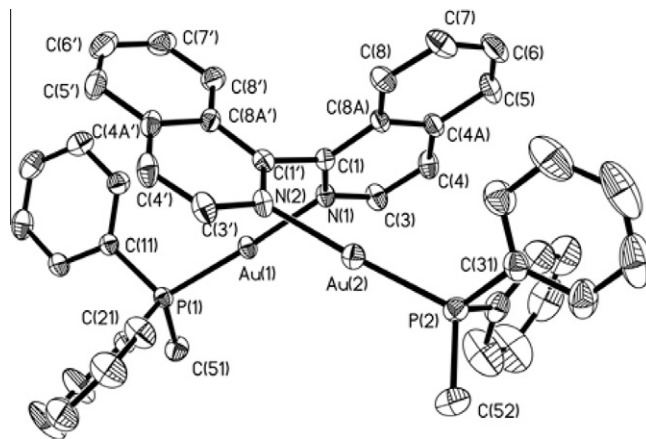


Fig. 3. Structure of the cation of compound **2c**. Displacement ellipsoids are at 25% probability level (H atoms omitted for clarity).

reported, namely [Pt(biisoq)(dapy)₃](ClO₄)₂ (dapy = 4-(dimethylamino)pyridine), with 77.6° torsion angle [7a]. The torsion angle between the two isoquinoline moieties in **1b** is 100.3°. This torsion angle is very close to those reported for the free ligands 8,8'-dimethyl-1,1'-biisoquinoline and 1,1'-biisoquinoline *N,N'*-dioxide, and corresponds to an *anti* arrangement. In contrast, related derivatives with the planar ligand 2,2'-bipyridine, [Au(bipy)(PPh₃)]PF₆ [24] and [(P–P)(Aubipy)₂](ClO₄)₂ [25] (P–P = bis(bis(o-methoxyphenoxy)phosphino)(phenyl)amine) show tricoordinated gold with torsion angles smaller than 8° and two Au–N bond distances of 2.167 and 2.404 Å, and 2.247 and 2.250 Å, respectively.

3.2.2. Crystal structure of complexes **2a**, **2c**, and **2d**

Crystals of **2a**, **2c** and **2d** were obtained by slow diffusion of hexane in a solution of the complex in dichloromethane at –18 °C. The studies (Figs. 2–4 and Tables 4 and 5) confirm the

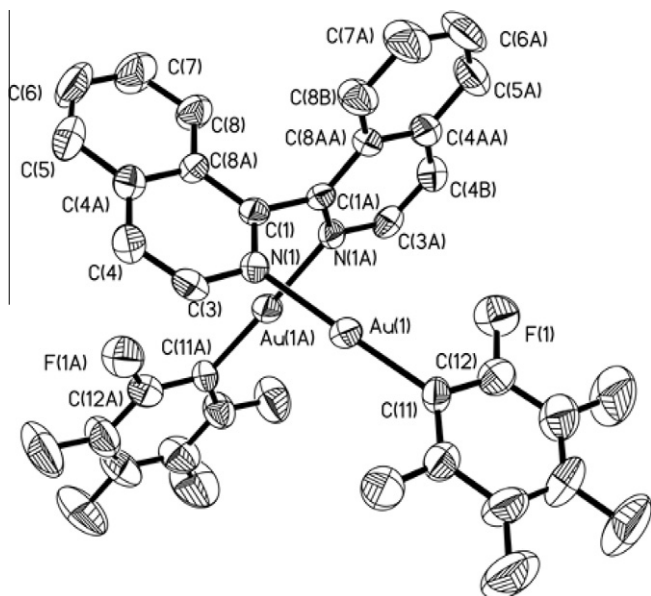


Fig. 4. Molecular structure of complex **2d**. Displacement ellipsoids are at 25% probability level (H atoms omitted for clarity).

Table 4
Selected bond lengths (Å) and angles (°) for the complex cations **2a** and **2c**.

	2a	2c
Au(1)–N(1)	2.116(6)	2.090(5)
Au(1)–P(1)	2.229(2)	2.2393(19)
Au(1)–Au(2)	3.0739(7)	4.505
N(1)–C(1)	1.326(11)	1.324(7)
P(1)–C	1.789(13)	1.777(6)
Au(2)–N(2)	2.115(8)	2.091(5)
Au(2)–P(2)	2.229(3)	2.231(2)
N(2)–C(1')	1.350(12)	1.339(7)
P(2)–C	1.772(13)	1.798(8)
N(1)–Au(1)–P(1)	176.2(2)	176.99(13)
N(2)–Au(2)–P(2)	175.3(2)	175.65(14)

Table 5
Selected bond lengths (Å) and angles (°) for **2d**.

Au(1)–N(1)	2.062(6)	C(11)–Au(1)–N(1)	179.0(3)
Au(1)–C(11)	2.003(8)	C(12)–C(11)–Au(1)	122.6(7)
N(1)–C(1)	1.316(9)	C(16)–C(11)–Au(1)	123.1(6)
N(1)–C(3)	1.388(10)	C(1)–N(1)–C(3)	118.4(6)
C(11)–C(12)	1.362(11)	C(1)–N(1)–Au(1)	122.2(5)
C(11)–C(16)	1.374(12)		

expected binuclear structure with a bridging bisoquinoline for both derivatives. The previous examples of this coordination mode were: (a) the two enantiomers of $[(\mu\text{-Cl})(\mu\text{-biisoq})\{\text{Pd}(\text{C-N})\}_2]\text{ClO}_4$ (C–N = 2-((*N,N*-dimethylamino)ethyl)phenyl-C,N), which show a torsion angle of 88.3° [11]; (b) the double bisoquinoline bridged silver (I) compounds $[(\mu\text{-biisoq})_2\{\text{Ag}(\text{OSO}_2\text{CF}_3)(\text{acetone})\}_2]$ and $[(\mu\text{-biisoq})_2(\text{AgXL})_2]$ (L = PPh₃, PMePh₂; X = CF₃SO₃, ClO₄) with torsion angles in the range 66.0–100.3°; (c) a single bridged silver (I) polymer $[(\mu\text{-biisoq})\text{Ag}(\text{OH}_2)_2(\mu\text{-biisoq})\text{Ag}]_n(\text{CF}_3\text{SO}_3)_{2n}$ with a torsional angle of 111.8°; (d) and finally, the related single bisoquinoline bridge of two phosphino-silver (I) units $[(\mu\text{-biisoq})\{\text{Ag}(\text{OSO}_2\text{CF}_3)(\text{PPh}_3)\}\{\text{Ag}(\text{OH}_2)(\text{PPh}_3)\}](\text{CF}_3\text{SO}_3)$ which displays a torsion angle of 113.1° and a long intramolecular silver–silver distance of 5.1557 Å [12].

The main difference between the three binuclear structures studied here is the torsion angle between the two isoquinoline moieties (65.2° for **2a**; 95.6° for **2c**; 80.1° for **2d**) which leads to

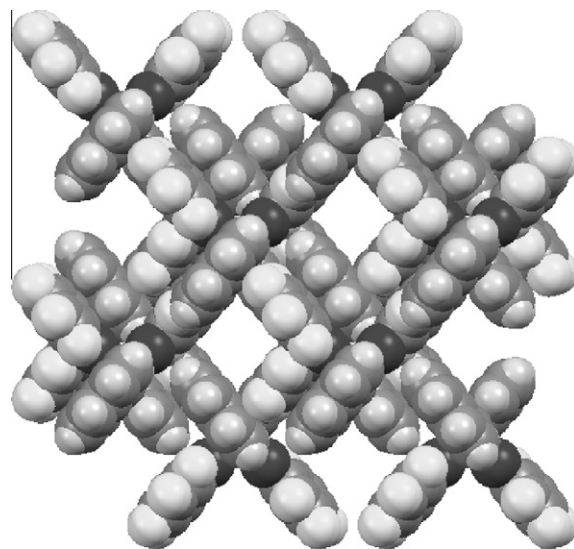


Fig. 5. View of the crystal packing of **2d** from the *c* axis (axes *a* and *b* in the plane). Spacefill representation.

Table 6
Normalized hydrogen bonds for complex **2d** (Å and °) [33].

C–H...F	d(C–H)	d(H...F)	d(C...F)	<(CHF)
C3–H3...F1#1	1.089	2.259	3.250	150.20
C5–H5...F2#2	1.089	2.551	3.302	125.31
C7–H7...F1#3	1.089	2.500	3.491	150.68
C7–H7...F5#4	1.089	2.519	3.346	131.89
C8–H8...F4#4	1.089	2.518	3.557	159.23
F1...H3–C3#5	1.089	2.259	3.250	150.20
F1...H7–C7#6	1.089	2.500	3.491	150.68
F2...H5–C5#7	1.089	2.551	3.302	125.31
F4...H8–C8#8	1.089	2.518	3.557	159.23
F5...H7–C7#8	1.089	2.519	3.346	131.89

Symmetry transformations used to generate equivalent atoms: #1 $x, 1 - y, -1/2 + z$; #2 $-1/2 + x, -1/2 + y, -1 + z$; #3 $-1/2 + x, 1/2 - y, -1/2 + z$; #4 $-1/2 + x, -1/2 + y, z$; #5 $x, 1 - y, 1/2 + z$; #6 $1/2 + x, 1/2 - y, 1/2 + z$; #7 $1/2 + x, 1/2 + y, 1 + z$; #8 $1/2 + x, 1/2 + y, z$.

Table 7
Electronic absorption data for the bisoquinoline ligand and the gold complexes^a.

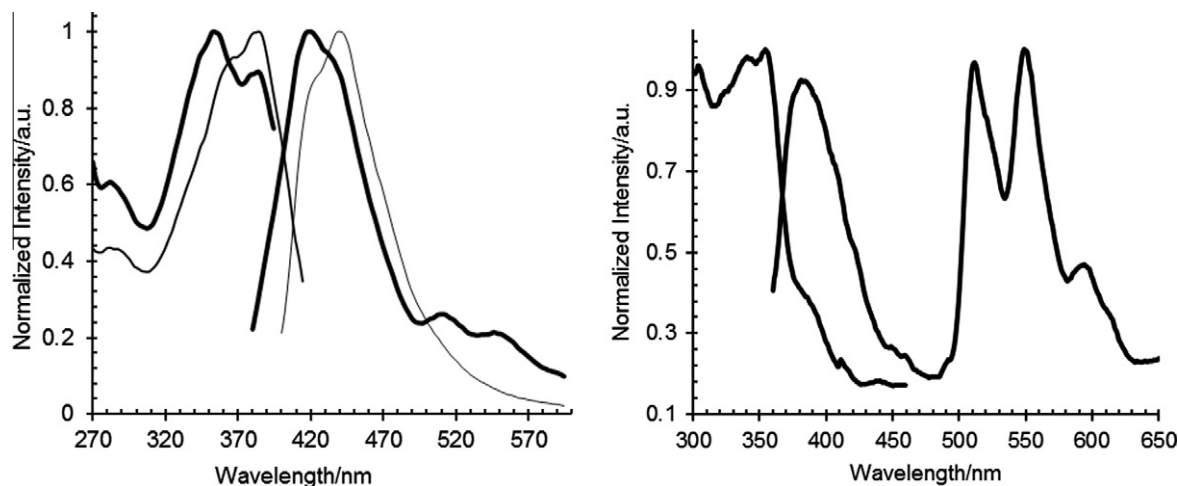
Derivative	λ/nm	$\epsilon/\text{M}^{-1} \text{cm}^{-1}$
biisoq	234 (31510), 279 (9110), 311 sh (6540), 322 (7930)	
2a	234 (62815), 278 (8123), 325 (7550), 338 sh (6405)	
2b	234 (109135), 267 (16705), 275 (14060), 326 (7330), 337 sh (5890)	
2c	232 (107060), 266 (12775), 274 (11175), 335 (7731)	
1b	233 (81060), 268 (11050), 275 (9650), 326 (7140) 336 sh (6165)	
2d–1d	228 (66825), 264 sh (17060), 284 sh (12055), 323 (8685), 334 sh (7150)	

^a In CH₂Cl₂ solution, ca. 5×10^{-5} M.

different values for the short intramolecular gold–gold distance: 3.0739(7) Å for **2a**; 4.505 Å for **2b**; and 3.785 Å for **2d**). There is an almost linear correspondence between the torsion angles and the gold–gold distances. The later suggest typical auriphilic interactions for **2a**; a distance slightly above the limits of auriphilic interactions (typically in the range 2.8–3.6 Å) for **2d**; and a clearly non-bonding intramolecular gold–gold distance for **2c**. These differences can be easily explained for **2a** and **2c**, which bear less sterically demanding phosphines and stabilize the usually less stable *syn* atropisomer. In contrast **2c**, with the bulkier phosphine, because of steric hindrance with the bulky phosphine, prefers the *anti* arrangement.

Table 8Excitation and emission data (in nm) in the solid state and in solution for the 1,1'-biisoquinoline and the gold derivatives **2a**, **2b**, **2c** and **1b**.

Comp.	Solid		Solid		CH ₂ Cl ₂	298 K		CH ₂ Cl ₂	77 K
	λ_{exc}	λ_{emis}	λ_{exc}	λ_{emis}		λ_{exc}	λ_{emis}		
biisoq	291, 341 ^a	400	292, 340 ^a	398	351	444		283, 336 ^a	388
2a	325	397 ^a , 422	295 ^a , 325, 340	429	328, 340 sh	391 ^a , 514, 545		341	372, 510 ^a , 548 ^a , 592
2b	296, 334 ^a	390	294 ^a , 326	370	367sh, 384(354 ^a , 381) ^b	423 sh, 440(419 ^a , 434sh, 511, 546) ^b		340, 354	382 ^a , 511 ^a , 549 ^a , 594
2c	364	411	296, 354 ^a	417	332	381 ^a , 451, 509		355	388, 511 ^a , 550 ^a , 593
1b	–	–	283 ^a , 322	426, 438 ^a	351(334) ^b	458(392, 451) ^b		334	389

^a Most intense peak.^b In parentheses: the second excitation and emission spectrum with less intensity.**Fig. 6.** Excitation and emission spectra in dichloromethane of complex **2b**: left at 298 K (recorded with two different excitation frequencies); right at 77 K.

A different interplay of forces operates in complex **2d**, where the structure is basically forced by the π – π stacking of C₆F₅ and isoquinoline rings, which leads to a N–C1–C1'–N' torsion angle of 80.1°. Moreover, this arrangement gives rise to the formation of channels in the crystal structure, as shown in Fig. 5. This specific arrangement can be related to the presence of intermolecular contacts between both ligands. Actually, there are five donor and five acceptor C–H...F weak non-classical hydrogen bonds per asymmetric unit (double for each molecule) as shown in Table 6. This combination of forces could overcome the alternative possibility of forming Au...Au interactions at a shorter distance.

3.3. Photophysical studies

The absorption spectra in dichloromethane were measured in the range 200–600 nm. The results are summarized in Table 7. The main spectral features for the gold complexes are: (a) an intense absorption at 230 nm due to phenyl rings [26]; (b) an absorption around 260–280 nm (a tail for mixture **2d–1d**) also related with the aromatic rings of the biisoquinoline, phosphine or pentafluorophenyl ligands; (c) a broad peak with intensity maxima in the range 325–335 nm, which is constituted by one absorption related to π – π^* transitions in the biisoquinoline ligand, and a second related tentatively to a charge transfer.

The emission and excitation spectra of the free ligand and the gold complexes were determined in the solid-state and in CH₂Cl₂ solution, at 298 and 77 K. The results are summarized in Table 8 and the spectra of complex **2b** are shown in Fig. 6. All the compounds, including the free 1,1'-biisoquinoline ligand, emit at 77 and 298 K in the solid state and in solution, with the only exception of **1b** in the solid state at 298 K; moreover, the mixture of **2d–1d**

did not emit, neither in solution nor in the solid state, even at 77 K. The later result confirms the electronic differences between pyridine and biisoquinoline, since a series of intensely luminescent pyridine halophenyl gold(I) complexes has been reported, with the emissions assigned to Ligand (halophenyl)–Metal to Ligand (pyridine) Charge Transfer transitions [27].

In the solid state, the emission range goes from 390 to 422 nm at 298 K, and from 370 to 438 nm at 77 K. The low temperature emission spectra are slightly blue (for **2b**, containing PPh₃) or red (for **2a** and **2c**, with PMe₃ and PPh₂Me, respectively) shifted, while the excitation spectra are similar with some small blue shifts. The biisoquinoline ligand is luminescent as expected from the presence of naphthalene-type units. In the solid state it is reasonable to assign the emission observed as ligand-centered modified by the gold phosphine moiety. The influence of Au...Au interactions in compound **2a**, if any, is not very relevant, contrarily to other phosphine–gold dimers as [Au₂(μ -dcpm)₂(ClO₄)₂] (dcpm = bis(dicyclohexylphosphine)methane) [28]. Dinuclear gold(I) compounds containing diphosphine and bipyridine ligand have been reported to show intense luminescence coming from the gold–bipyridine unit, where the large spin–orbit coupling of the Au 5d electrons facilitates the emission [29].

Comparing for each compound the spectra in the solid state and in solution, these are clearly different (Table 8). The typical red shift on going from solution to the solid state, which is a common effect in the emission spectra of gold(I) complexes due to intermolecular Au...Au interactions, is not observed. In fact, the spectra in CH₂Cl₂ solution are more complicated than in the solid state, with emission maxima in the range 381–458 nm (or 546 nm considering low intensity emissions) at 298 K, whereas they are luminescent at 77 K in the range 382–550 nm. The low temperature

emission maxima are strongly blue (for bisoquinoline and **1b**) or red (for **2a–2c**) shifted; in the last case the low intensity bands at 298 K become the most intense ones at 77 K. The excitation spectra are similar with some small blue (for bisoquinoline, **2b** and **1b**) or red (for **2a** and **2c**) shifts. At 77 K, all of them show a high energy emission around 390 nm, which could be directly related with the bisoquinoline ligand; moreover, dinuclear gold derivatives **2a–c** display a more intense low energy emission at 510, with vibronic progressions at 550 and 595 nm ($1319\text{--}1387\text{ cm}^{-1}$, close to those found in the IR spectra for skeletal vibrations in the bisoquinoline). These could be tentatively assigned as a charge transfer involving the bisoquinoline ligand, because it is only visible in the compounds containing a digold fragment (**2a**, **2b** and **2c**; the three spectra are quite similar independently of the phosphine used). A MLCT has been also proposed for some luminescent bipy phosphino gold(I) derivatives [30,31]. Theoretical studies by Time-Dependent Density-Functional Theory methods (TD-DFT) on some related compounds, and the presence of vibronic aromatic spacing, point out to emissions coming from $\pi\pi^*$ states of the aromatic core in: (a) mononuclear gold(I) complexes with 4-substituted pyridines $[\text{Au}(4\text{-dmapy})_2][\text{AuCl}_2]$ (dmapy = dimethylaminopyridine) and $[\text{Au}(4\text{-pic})_2][\text{AuCl}_2]$ [31]; (b) phosphino gold(I) derivatives of naphthalene, where it is also observed in some cases, a high energy emission and a low energy emission, showing the latter vibronic progressions [32].

4. Conclusions

The torsion angle between the two isoquinoline units is typically around 100° for the free ligand or related ligands. This could be considered the natural angle when no other forces operate. A similar angle is found in our monodentate 1,1'-bisquinoline complex. However, this flexible ligand, can modify the N–N distance and the bonding orientation of the lone pair by changing the torsion angle between the two isoquinoline units, allowing for monodentate or bidentate, bridging or chelating modes in metal complexes. Within the limits of this flexibility, the preferred structure is also determined by the steric requirements of the metallic fragment, the possible aurophilic interactions and, in the solid state, even by the influence of multiple weaker intermolecular contacts. In the cases studied here the torsion angles and the intramolecular gold–gold distances are 100.32° for the mononuclear **1b**; 65.2° and $3.0739(7)\text{ \AA}$ for the dinuclear **2a**, 80.10° and 3.785 \AA for the dinuclear **2d**, 95.6° and 4.505 \AA for the dinuclear **2c**. Most derivatives are luminescent at room temperature in the solid state and in solution. In frozen dichloromethane at 77 K, the phosphino digold compounds display a dual emission, the low energy one shows bisoquinoline vibronic progressions.

Acknowledgments

We thank the Spanish Comisión Interministerial de Ciencia y Tecnología (Project CTQ2011-25137) and the Junta de Castilla y León (Project VA248A11-2) for financial support.

Appendix A. Supplementary material

CCDC 857019–857022 contain the supplementary crystallographic data for compounds **1b**, **2a**, **2c** and **2d**. These data can be obtained free of charge from The Cambridge Crystallographic Data Centre via www.ccdc.cam.ac.uk/data_request/cif. Supplementary data associated with this article can be found, in the online version, at <http://dx.doi.org/10.1016/j.ica.2012.06.024>.

References

- [1] (a) H. Schmidbaur, A. Schier, *Chem. Soc. Rev.* 41 (2012) 370; (b) J. Muñoz, C. Wang, P. Pykkö, *Chem. Eur. J.* 17 (2011) 368; (c) P. Pykkö, *Chem. Soc. Rev.* 37 (2008) 1967.
- [2] (a) D.M. Roundhill, J.P. Fackler Jr., *Optoelectronic Properties of Inorganic Compounds*, Plenum Press, New York, 1998; (b) R.B. Thomas, P.A. Smith, A. Jaleel, P. Vogel, C. Crawford, Z. Assefa, R.E. Sykora, *Inorg. Chem.* 51 (2012) 3399; (c) H.E. Abdou, A.A. Mohamed, J.M. López de Luzuriaga, M. Monge, J.P. Fackler Jr., *Inorg. Chem.* 51 (2012) 2010; (d) A.L. Balch, *Angew. Chem., Int. Ed.* 48 (2009) 2641; (e) E.R.T. Tiekink, J.-G. Kang, *Coord. Chem. Rev.* 253 (2009) 1627; (f) H. Ito, T. Saito, N. Oshima, N. Kitamura, S. Ishizaka, Y. Hinatsu, M. Wakeshima, M. Kato, K. Tsuge, M. Sawamura, *J. Am. Chem. Soc.* 130 (2008) 10044; (g) Y.A. Lee, R. Eisenberg, *J. Am. Chem. Soc.* 125 (2003) 7778; (h) J.C. Vickery, M.M. Olmstead, E.Y. Fung, A.L. Balch, *Angew. Chem., Int. Ed.* 36 (1997) 1179.
- [3] (a) X. He, V.W.W. Yam, *Coord. Chem. Rev.* 255 (2011) 2111; (b) X. He, F. Herranz, E.C.C. Cheng, R. Vilar, V.W.W. Yam, *Chem. Eur. J.* 16 (2010) 9123; (c) S.K. Yip, E.C.C. Cheng, L.H. Yuan, N. Zhu, V.W.W. Yam, *Angew. Chem., Int. Ed.* 43 (2004) 4954; (d) C. Fave, T.Y. Cho, M. Hissler, C.W. Chen, T.Y. Luh, C.C. Wu, R. Réau, *J. Am. Chem. Soc.* 125 (2003) 9254; (e) E.J. Fernández, J.M. López-de-Luzuriaga, M. Monge, M.E. Olmos, J. Pérez, A. Laguna, A.A. Mohamed, J.P. Fackler, *J. Am. Chem. Soc.* 125 (2003) 2022; (f) Y. Ma, C.M. Che, H.Y. Chao, X. Zhou, W.H. Chan, J. Shen, *Adv. Mater.* 11 (1999) 852; (g) M.A. Mansour, W.B. Connick, R.J. Lachicotte, H.J. Gysling, R. Eisenberg, *J. Am. Chem. Soc.* 120 (1998) 1329.
- [4] (a) K. Wilckens, D. Lentz, C. Czekelius, *Organometallics* 30 (2011) 1287; (b) M. Hatano, K. Ishihara, *Synthesis* (2010) 3785; (c) Z. Liu, M. Shi, *Organometallics* 29 (2010) 2831; (d) J. Ruan, G. Lu, L. Xu, Y.-M. Li, A.S.C. Chan, *Adv. Synth. Catal.* 350 (2008) 76; (e) D. Baskakov, W.A. Herrmann, E. Herdtweck, S.D. Hoffmann, *Organometallics* 26 (2007) 626; (f) W.A. Herrmann, D. Baskakov, E. Herdtweck, S.D. Hoffmann, T. Bunlaksananusorn, F. Rampf, L. Rodefeld, *Organometallics* 25 (2006) 2449.
- [5] (a) E.L. Eliel, S.H. Wilen, L.N. Mander, *Stereochemistry of Organic Compounds*, Wiley, New York, 1994; (b) M.T. Ashby, G.N. Govindan, A.K. Grafton, *J. Am. Chem. Soc.* 116 (1994) 4801.
- [6] K. Yamamoto, H. Tateishi, K. Watanabe, T. Adachi, H. Matsubara, T. Ueda, T. Yoshida, *Chem. Commun.* (1995) 1637.
- [7] (a) L.-K. Cheng, K.-S. Yeung, C.-M. Che, M.-C. Cheng, Y. Wang, *Polyhedron* 12 (1993) 1201; (b) C.-Y. Kuo, M.-J. Wu, C.-C. Lin, *Eur. J. Med. Chem.* 45 (2010) 55.
- [8] (a) M.T. Ashby, *J. Am. Chem. Soc.* 117 (1995) 2000; (b) E.C. Glazer, S.S. Alguindigue, M.A. Khan, *Organometallics* 19 (2000) 547; (c) M.T. Ashby, S.S. Alguindigue, J.D. Schwane, T.A. Daniel, *Inorg. Chem.* 40 (2001) 6643.
- [9] (a) M.T. Ashby, C.N. Govindan, A.K. Grafton, *Inorg. Chem.* 32 (1993) 3803; R. Yang, L. Dai, *Chin. Chem. Lett.* 4 (1993) 1021; (c) W.-Y. Yu, W. Cheng, C.-M. Che, Y. Wang, *Polyhedron* 13 (1994) 2963; (d) E.C. Glazer, Y. Tor, *Angew. Chem., Int. Ed.* 41 (2002) 4022; (e) E. Baranoff, J.-P. Collin, J. Furusho, Y. Furusho, A.-C. Laemmel, J.-P. Sauvage, *Inorg. Chem.* 41 (2002) 1215; (f) P. Fredani, C. Gianelli, A. Salvini, S. Ianelli, *J. Organomet. Chem.* 667 (2003) 197.
- [10] Q. Zhao, S. Liu, M. Shi, C. Wang, M. Yu, L. Li, F. Li, T. Yi, C. Huang, *Inorg. Chem.* 45 (2006) 6152.
- [11] L.X. Dai, Z.H. Zhou, Y.Z. Zhang, C.I. Ni, Z.M. Zhang, Y.F. Zhou, *Chem. Commun.* (1987) 1760.
- [12] M. Bardají, A.B. Miguel-Coello, P. Espinet, *Inorg. Chim. Acta* 386 (2012) 93.
- [13] H. Schmidbaur, A. Wohlleben, F. Wagner, O. Orama, G. Huttner, *Chem. Ber.* 110 (1977) 1748.
- [14] R. Usón, A. Laguna, J. Vicente, *Chem. Commun.* (1976) 353.
- [15] SMART V5.051, Software for the CCD Detector System; Bruker Analytical X-ray Instruments Inc., Madison, WI, 1998.
- [16] SAINT V6.02, Integration Software, Bruker Analytical X-ray Instruments Inc., Madison, WI, 1999.
- [17] G.M. Sheldrick, SADABS: A Program for Absorption Correction with the Siemens SMART System, University of Göttingen, Göttingen, Germany, 1996.
- [18] SHELXTL program system version 5.1, Bruker Analytical X-ray Instruments Inc., Madison, WI, 1998.
- [19] G. Dyker, W. Stirner, G. Henkel, P.R. Schreiner, *Helv. Chim. Acta* 91 (2008) 904.
- [20] H. Tsue, H. Fujinami, T. Itakura, R. Tsuchiya, K. Kobayashi, H. Takahashi, K. Hirao, *Chem. Lett.* (1999) 17.
- [21] M. Nakajima, M. Saito, M. Shiro, S. Hashimoto, *J. Am. Chem. Soc.* 120 (1998) 6419.
- [22] M. Bardají, M. Barrio, P. Espinet, *Dalton Trans.* 40 (2011) 2570.
- [23] J.E. Aguado, M.J. Calhorda, M.C. Gimeno, A. Laguna, *Chem. Commun.* (2005) 3355.

- [24] W. Clegg, *Acta Crystallogr., Sect. B: Struct. Crystallogr. Cryst. Chem.* 32 (1976) 2712.
- [25] C. Ganesamoorthy, M.S. Balakrishna, J.T. Mague, H.M. Tuononen, *Inorg. Chem.* 47 (2008) 2764.
- [26] C. King, J.-C. Wang, M.N.I. Khan, J.P. Fackler Jr., *Inorg. Chem.* 28 (1989) 2145.
- [27] E.J. Fernández, A. Laguna, J.M. López de Luzuriaga, M. Monge, M. Montiel, M.E. Olmos, J. Pérez, M. Rodríguez-Castillo, *Gold Bull.* 40 (2007) 172.
- [28] K.H. Leung, D.L. Phillips, M.-C. Tse, C.-M. Che, V.M. Miskowski, *J. Am. Chem. Soc.* 121 (1999) 4799.
- [29] P.-S.G. Kim, Y. Hu, M.-C. Brandys, T.J. Burchell, R.J. Puddephatt, T.K. Sham, *Inorg. Chem.* 46 (2007) 949.
- [30] M.-C. Brandys, M.C. Jennings, R.J. Puddephatt, *J. Chem. Soc., Dalton Trans.* (2000) 4601.
- [31] J.C.Y. Lin, S.S. Tang, C. Sekhar Vasam, W.C. You, T.W. Ho, C.H. Huang, B.J. Sun, C.Y. Huang, C.S. Lee, W.S. Hwang, A.H.H. Chang, I.J.B. Lin, *Inorg. Chem.* 47 (2008) 2543.
- [32] (a) D.V. Partyka, M. Zeller, A.D. Hunter, T.G. Gray, *Angew. Chem., Int. Ed. Engl.* 25 (2006) 8188;
(b) L. Gao, M.A. Peay, D.V. Partyka, J.B. Updegraff III, T.S. Teets, A.J. Esswein, M. Zeller, A.D. Hunter, T.G. Gray, *Organometallics* 28 (2009) 5669.
- [33] C.F. Macrae, I.J. Bruno, J.A. Chisholm, P.R. Edgington, P. McCabe, E. Pidcock, L. Rodriguez-Monge, R. Taylor, J. van de Streek, P.A. Wood, *J. Appl. Crystallogr.* 41 (2008) 466.